Proc. Natl. Acad. Sci. USA
Vol. 87, pp. 1942–1946, March 1990
Biochemistry

Structural analysis of the $(dA)_{10}\cdot 2(dT)_{10}$ triple helix

(UV mixing curve/helix–coil transition/imino proton NMR/nuclear Overhauser effect spectroscopy/Hoogsteen base pair)

DANIEL S. PILCH*, COREY LEVENSON†, AND RICHARD H. SHAFER‡§

*Graduate Group in Biophysics and ‡Department of Pharmaceutical Chemistry, School of Pharmacy, University of California, San Francisco, CA 94143; and †Cetus Corporation, Emeryville, CA 94608

Communicated by I. Tinoco, Jr., December 26, 1989

ABSTRACT **The existence of DNA triple helices *in vitro* has been known for some time. Recent evidence suggesting that DNA triplexes exist *in vivo* and showing their potential for chemotherapeutic applications has renewed interest in these triple-stranded conformations. However, little structural information is currently known about these unusual nucleic acid forms. We have induced and stabilized triple-helical $(dA)_{10}\cdot 2(dT)_{10}$ with $MgCl_2$ at neutral pH. UV mixing curves demonstrate a 1:2 $(dA)_{10}$ to $(dT)_{10}$ stoichiometry at suitable $MgCl_2$ concentrations. Thermal denaturation profiles establish a melting mechanism characterized by the initial loss of the third strand, followed by dissociation of the remaining duplex. The circular dichroic spectrum of the triplex form is distinct from that of a duplex equimolar in $(dA)_{10}$. NMR studies show that magnesium-induced triplex formation is accompanied by an upfield shift of several imino proton resonances present before stabilization of the triplex form with $MgCl_2$ and the induction of new upfield imino proton resonances. Nuclear Overhauser effect spectroscopy measurements on both undeuterated and C8—H-deuterated $(dA)_{10}\cdot 2(dT)_{10}$ triplexes demonstrate dipolar contacts between resolvable imino proteins and both adenine C8—H and C2—H aromatic protons. Hence, $MgCl_2$ stabilizes a triplex structure in which thymine N3—H imino protons are involved in both Watson–Crick and Hoogsteen base pairing.**

Although the triple-helix form of nucleic acids containing homopurine–homopyrimidine sequences has been known for several decades (1–3), interest has recently been generated in this structure because of data showing its potential biological significance. The work of Frank-Kamenetskii and coworkers (4) on the H form of DNA has spurred much of this interest. Their structural model explains the S1 nuclease sensitivity observed in plasmids containing $(dC\text{-}dT)_n\cdot(dA\text{-}dG)_n$ sequences by invoking the formation of triple-helical regions, with a single strand looped out and, hence, susceptible to single-strand-specific endonucleases. In addition, the work of Moser and Dervan (5) and Praseuth *et al.* (6) on sequence-specific DNA binding and cutting agents based on triple-helix formation has established the potential for therapeutic applications based on this particular nucleic acid form through gene regulation. This potential has been explored in studies on the inhibition of c-*myc* expression *in vitro* by triple-helix formation (7).

Until recently, the only structural information available on the triple helix was derived from polynucleotide fiber diffraction studies (8–10). These studies have resulted in a model of the triple helix in which the third strand lies in the major groove of the underlying duplex. The extra strand interacts with the other two by means of Hoogsteen base pairing. In addition, the duplex portion of the structure takes on an A-like conformation, with C3′-*endo*(^3E) sugar pucker. The third strand can be either homopurine or homopyrimidine, depending on pH and other conditions, although more data are available on systems containing a third pyrimidine strand. In such cases, the third strand is parallel to the purine strand. The question of strand polarity has been addressed further experimentally by both Praseuth *et al.* (6) and Moser and Dervan (5). The sequence specificity of triple-helix formation has been studied experimentally by Fresco and coworkers (11).

NMR studies have been recently reported on both octamer (12, 13) and 11-mer (14) triplexes containing both T·A·T and $C\cdot G\cdot C^+$ base triplets and stabilized by low pH and/or $MgCl_2$. In the work presented below, we describe experiments probing the structure and stability of the Mg^{2+}-induced triplex $(dA)_{10}\cdot 2(dT)_{10}$ at neutral pH. UV mixing curves establish the 1:2 purine-to-pyrimidine stoichiometry, and thermal denaturation profiles show the initial loss of the third strand, followed by dissociation of the duplex form. Circular dichroic spectra of both the duplex and triplex forms of this system are presented, and NMR experiments demonstrate both Watson–Crick (W–C) and Hoogsteen base pairing in the triplex form.

MATERIALS AND METHODS

In this communication, the colon [as in $(dA)_{10}$:$2(dT)_{10}$] denotes a stoichiometric ratio of two DNA strands. The minibullet [as in $(dA)_{10}\cdot 2(dT)_{10}$] denotes an actual DNA structure, such as triplex or duplex.

Chemicals and Oligodeoxynucleotides. The oligomers $(dA)_{10}$ and $(dT)_{10}$ were synthesized on a preparative DNA synthesizer (MilliGen/Biosearch 8800) by standard cyanoethylphosphoramidite chemical methods. After deprotection with NH_4OH, the crude oligomers were purified by anion-exchange HPLC (Zorbax-Oligo column from DuPont, 4.7 mm i.d. to 10 cm). HPLC purifications were run isocratically at a flow rate of 2 ml/min. The following buffers were used: buffer A was 30% (vol/vol) acetonitrile/20 mM aqueous sodium acetate (pH 7.6). Buffer B was the same as buffer A but contained 1 M LiCl. Elution conditions were 78% buffer A plus 22% buffer B for $(dT)_{10}$ and 82% buffer A plus 18% buffer B for $(dA)_{10}$. Retention time was ≈6 min in both cases, with ≥98% of the absorbance at 254 nm appearing as a single peak. The oligomers were then dialyzed against 2 mM sodium phosphate (pH 7.1) and their purity was checked by ^1H NMR. Concentrations of $(dA)_{10}$ and $(dT)_{10}$ were determined spectrophotometrically; the reported extinction coefficients for poly(dA) [ε_{257} = 8600 cm^{-1}(mole base/liter)$^{-1}$] (15) and poly(dT) [ε_{265} = 8700 cm^{-1}(mole base/liter)$^{-1}$] (2), respectively, were used. All oligomer concentrations, except where noted otherwise, are reported on a strand basis. D_2O was purchased from Cambridge Isotope Laboratories (Cambridge, MA), and all other buffer reagents were from Sigma.

The publication costs of this article were defrayed in part by page charge payment. This article must therefore be hereby marked "*advertisement*" in accordance with 18 U.S.C. §1734 solely to indicate this fact.

Abbreviations: NOE, nuclear Overhauser enhancement; NOESY, (2D) NOE spectroscopy; W–C, Watson–Crick.

§To whom reprint requests should be addressed.

UV Mixing Curves. Mixing curves for the interactions of $(dA)_{10}$ and $(dT)_{10}$ were determined by using the method of continuous variations (16). Equimolar solutions of $(dA)_{10}$ and $(dT)_{10}$ were made in 10 mM sodium phosphate (pH 7.1) and either 50 mM $MgCl_2$ or 100 mM NaCl. Aliquots (25–200 μl) of $(dT)_{10}$ were added to 200 μl of $(dA)_{10}$ in a quartz cuvette (1-cm path length). For mixing, the covered cuvette was repeatedly inverted after each addition, and the mixture was allowed to equilibrate for 10 min at 5°C. After equilibration, absorbance of the solution was measured at 260 nm and 5°C in a Gilford 2600 spectrophotometer equipped with a Gilford 2527 thermoprogrammer. The cuvette-holding chamber was flushed with a constant stream of N_2 gas to avoid water condensation on the cuvette exterior.

t_m Determinations. Equimolar (11 μM) solutions of $(dT)_{10}$ and $(dA)_{10}$ in 10 mM Tris·HCl (pH 7.3)/50 mM $MgCl_2$ were combined to give mixtures with final stoichiometric ratios of either 1:1 or 1:2 $(dA)_{10}$ to $(dT)_{10}$. The absorbance of each mixture was measured once per minute at wavelengths of 260 and 284 nm in the Gilford 2600 spectrophotometer. The temperature was increased at a rate of 0.25°C/min, and the total run time was 260 min. The cuvette-holding chamber was flushed with N_2 gas for the duration of the run.

Circular Dichroism (CD). Equimolar (11 μM) solutions of $(dA)_{10}$ and $(dT)_{10}$ in 10 mM sodium phosphate (pH 7.1)/50 mM $MgCl_2$ were combined to give mixtures with stoichiometric ratios of either 1:1 or 1:2 $(dA)_{10}$ to $(dT)_{10}$. The ellipticities of these mixtures, as well as those of $(dA)_{10}$ and $(dT)_{10}$ alone, were measured from 220 to 340 nm in a Jasco J-500A spectropolarimeter. The temperature was held at 5°C for all measurements by using a Fisher 9000 circulating water bath.

Deuterium Exchange of Adenine C8—H. A solution (0.76 mM) of $(dA)_{10}$ in 25 mM sodium phosphate (pH 8.0) was lyophilized to dryness and resuspended in an equal volume of 99.97% D_2O. The resulting solution was incubated for 10 hr at 89°C in a sealed microcentrifuge tube. The sample was then dialyzed against 2 mM sodium phosphate (pH 7.1), lyophilized, and resuspended in an equal volume of 99.97% D_2O. The extent of deuteration was checked by ^1H NMR.

Imino Proton NMR. All NMR experiments were done on a 500-MHz General Electric GN-500 spectrometer equipped with an Oxford Instruments magnet and a Nicolet 1280 computer. Imino proton NMR measurements were made on 400 μl of solution containing 2 mM $(dT)_{10}$ and 1 mM of either undeuterated or C8—H-deuterated $(dA)_{10}$ in aqueous phosphate buffer [10 mM sodium phosphate (pH 7.1) in 10% D_2O/90% H_2O]. Aliquots of 0.5 M $MgCl_2$ were added to a final concentration of 10 mM, and the imino proton spectrum was acquired after each addition. The net dilution resulting from addition of the $MgCl_2$ was ≈2%. The imino proton spectra were obtained by using the solvent suppression $1\bar{3}3\bar{1}$ pulse sequence (17) with the carrier frequency set at the H_2O resonance. An interval delay, τ, of 96 μsec was used along with a pulse repetition time of 3 sec. Temperature was fixed at 11°C.

Imino Proton–Aromatic Proton Nuclear Overhauser Effect Spectroscopy (NOESY) Experiments. Two-dimensional NOESY experiments were done on solutions containing 4 mM $(dT)_{10}$ and 2 mM of either undeuterated or C8—H-deuterated $(dA)_{10}$ [or 2 mM triplex $(dA)_{10}$·2$(dT)_{10}$] in 12 mM sodium phosphate (pH 7.1)/15 mM $MgCl_2$ in 10% D_2O/90% H_2O. Phase-sensitive NOESY spectra were acquired in the pure absorption mode (18). The exciting 90° pulse was replaced by a $1\bar{3}3\bar{1}$ pulse sequence, with the carrier frequency set at the H_2O resonance. A short homospoil pulse was applied at the start of the mixing time to suppress the H_2O signal (19). A mixing time of 250 msec was used along with an interval delay of 80 μsec and a 3-sec pulse repetition time. Temperature was fixed at 12°C. The data sets consisted of 4096 complex points in the t_2 dimension stored in alternating blocks with 16 scans for each of the 400 increments in the t_1 dimension. All spectra were acquired with a spectral width of 12,048 Hz in both dimensions. The free induction decays (FIDs) were apodized with a 130°-shifted sine-bell function in both dimensions and zero-filled once in each dimension before Fourier transformation. The baselines of the spectra were corrected to a sixth-order polynomial in both ω_1 and ω_2 (20, 21). Processing of the two-dimensional data sets was performed on a Sparc Station 1 (Sun Microsystems, Milpitas, CA) computer.

RESULTS AND DISCUSSION

UV Mixing Curves. The stoichiometries associated with the various interactions between $(dA)_{10}$ and $(dT)_{10}$ at differing cationic concentrations were determined from UV absorbance mixing curves with the method of continuous variation described in the preceding section. Fig. 1 shows the UV absorbance changes accompanying continuous addition of $(dT)_{10}$ to a fixed amount of $(dA)_{10}$ at cationic concentrations of either 100 mM NaCl (Fig. 1*A*) or 50 mM $MgCl_2$ (Fig. 1*B*). At 100 mM NaCl, the point of minimum absorbance (maximum hypochromicity) corresponds to an approximate 1:1 molar ratio [47% $(dT)_{10}$] of $(dA)_{10}$ to $(dT)_{10}$ (Fig. 1*A*). A cationic concentration of 100 mM NaCl is, therefore, only sufficient to allow duplex $(dA)_{10}$·$(dT)_{10}$ formation. In contrast, the point of minimum absorbance at 50 mM $MgCl_2$ corresponds to an approximate 1:2 molar ratio [63% $(dT)_{10}$] of $(dA)_{10}$ to $(dT)_{10}$ (Fig. 1*B*). Under these cationic conditions, formation and stabilization of triple-helical $(dA)_{10}$·2$(dT)_{10}$ is therefore indicated. Higher NaCl concentrations (e.g., 2.0 M) will also promote triplex formation (data not shown). The shape and stoichiometry of the mixing curves are identical regardless of which strand [$(dA)_{10}$ or $(dT)_{10}$] is used in fixed amounts (data not shown). Given the appropriate 1:2 stoichiometry of $(dA)_{10}$ to $(dT)_{10}$, these mixing experiments

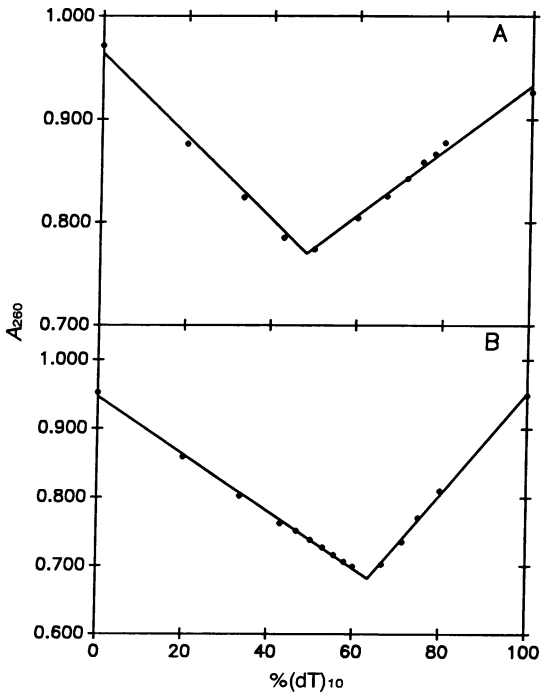

FIG. 1. UV mixing curves for reactions between $(dA)_{10}$ and $(dT)_{10}$ at either 100 mM NaCl (*A*) or 50 mM $MgCl_2$ (*B*). Mixing experiments were done in 10 mM sodium phosphate buffer (pH 7.1). Values on the abscissa are in mole %.

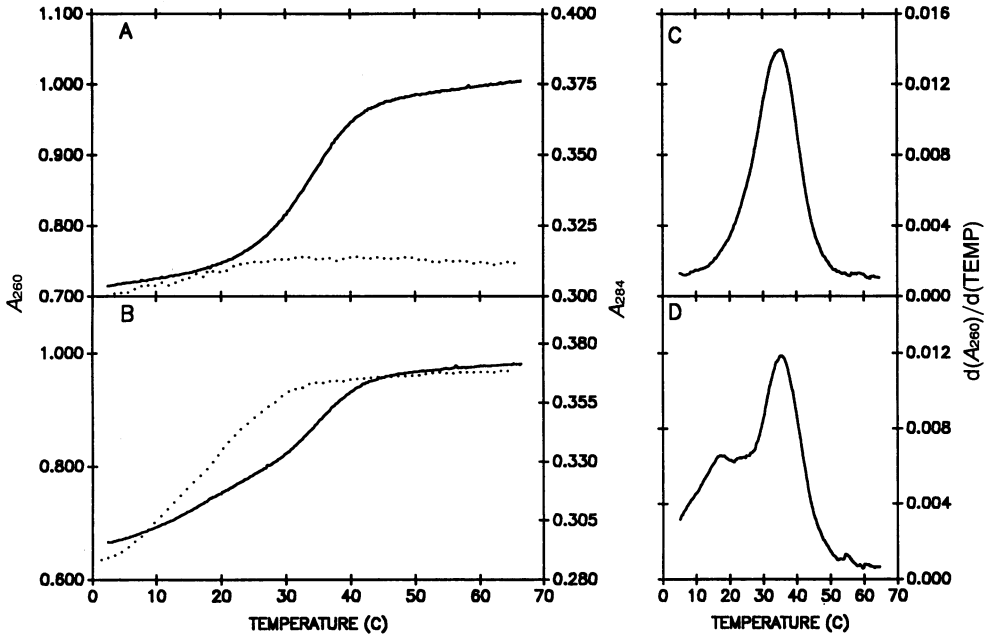

FIG. 2. Helix–coil transitions of solutions containing either 1:1 (*A* and *C*) or 1:2 (*B* and *D*) molar ratios of $(dA)_{10}$:$(dT)_{10}$ at 260 nm (——) and 284 nm (· · · ·). First-derivative plots of the 260-nm transitions are shown in *C* and *D*. Melting experiments were done in 10 mM Tris·HCl (pH 7.3)/50 mM $MgCl_2$. TEMP, temperature.

indicate that sufficiently high concentrations of Mg^{2+} (or Na^+) ions will stabilize the $(dA)_{10}$·$2(dT)_{10}$ triplex structure.

Helix–Coil Transitions. Additional evidence that a $(dA)_{10}$·$2(dT)_{10}$ triplex structure is stabilized in solution containing a 1:2 molar ratio of $(dA)_{10}$:$(dT)_{10}$ and 50 mM $MgCl_2$ was afforded by thermal denaturation studies. The UV absorption spectra of native and melted duplex $(dA)_{10}$·$(dT)_{10}$ at 50 mM $MgCl_2$ share a virtual isosbestic point at 284 nm. In contrast, the UV absorption spectra of triplex $(dA)_{10}$·$2(dT)_{10}$ and appropriately normalized duplex $(dA)_{10}$·$(dT)_{10}$ plus single-stranded $(dT)_{10}$, at this same salt concentration, do not share this isosbestic point (data not shown). Thus, melting of the third strand from the underlying duplex is accompanied by a hyperchromic absorbance change at 284 nm, whereas denaturation of the duplex W–C strands is not. Both of these events, however, are accompanied by hyperchromic absorbance changes at 260 nm.

The helix–coil transitions of solutions containing either 1:1 or 1:2 stoichiometric ratios of $(dA)_{10}$:$(dT)_{10}$ and 50 mM $MgCl_2$ at both 260 nm and 284 nm are shown in Fig. 2. At 50 mM $MgCl_2$, the $(dA)_{10}$:$(dT)_{10}$ solution has a monophasic helix–coil transition at 260 nm and no observable transition at 284 nm (Fig. 2*A*). Fig. 2*C* shows the first-derivative plot of the 260-nm transition and confirms its monophasic nature, yielding a t_m of 35.4 ± 0.4°C. This transition is therefore associated with denaturation of the duplex (W–C strands) only. In striking contrast, the helix–coil transition of the $(dA)_{10}$:$2(dT)_{10}$ solution is biphasic at 260 nm and monophasic at 284 nm (Fig. 2*B*). The biphasic nature of the 260-nm transition is much more evident in the first-derivative plot (Fig. 2*D*), which shows t_m values of 17.7 ± 0.5°C and 35.4 ± 0.4°C. The single transition present at 284 nm corresponds to the first of the two transitions at 260 nm with a t_m of 17.7 ± 0.5°C. Hence, the lower t_m (17.7°C) corresponds to the melting of the third strand from the underlying duplex, whereas the higher t_m (35.4°C) corresponds to the denaturation of the duplex as demonstrated above. These melting curves indicate that the structure resulting in the $(dA)_{10}$:$2(dT)_{10}$ solution is triple-helical in nature and that its melting mechanism may be given by the following equations:

$$(dA)_{10}\cdot 2(dT)_{10} \rightarrow (dA)_{10}\cdot(dT)_{10} + (dT)_{10} \rightarrow (dA)_{10} + 2(dT)_{10}.$$

CD. CD spectroscopy also confirms the presence of a unique structure in a solution containing a 1:2 molar ratio of $(dA)_{10}$:$(dT)_{10}$ and 50 mM $MgCl_2$. Fig. 3*A* compares the CD spectrum of a $(dA)_{10}$:$2(dT)_{10}$ solution with an appropriately normalized sum of spectra from $(dA)_{10}$:$(dT)_{10}$ plus $(dT)_{10}$ solutions at 50 mM $MgCl_2$. The former spectrum exhibits differences relative to the latter, which include a slight amplitude increase and red-shift of the negative band at 248 nm, a substantial amplitude decrease of the positive band at 280 nm, and an amplitude increase and red-shift of the positive band at 259 nm. Fig. 3*B* compares the CD spectrum of a $(dA)_{10}$:$2(dT)_{10}$ solution with that of a $(dA)_{10}$:$(dT)_{10}$ solution of the same $(dA)_{10}$ concentration. In this case, spectral distinctions of the former relative to the latter include an amplitude increase and slight red-shift of the

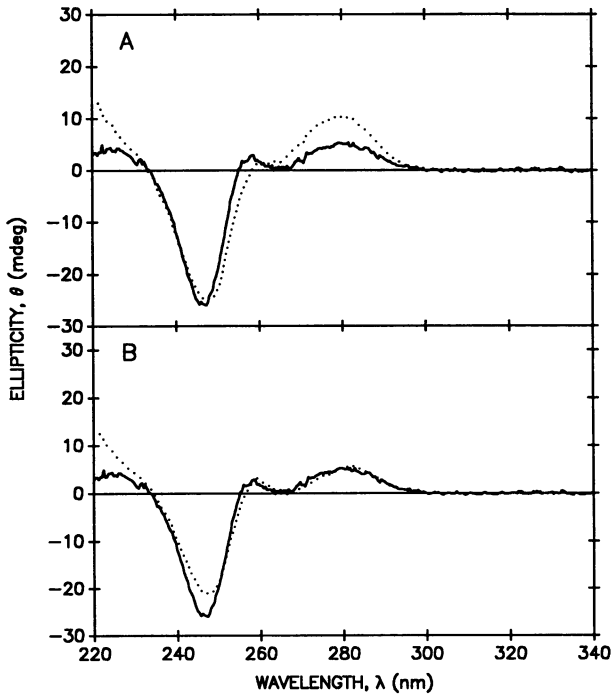

FIG. 3. CD spectrum of a $(dA)_{10}$:$2(dT)_{10}$ solution (——) compared with that of the normalized sum of a $(dA)_{10}$:$(dT)_{10}$ plus $(dT)_{10}$ solutions (· · · ·) (*A*) or with that of a $(dA)_{10}$:$(dT)_{10}$ solution equimolar in $(dA)_{10}$ (· · · ·) (*B*). The CD experiments were done in 10 mM sodium phosphate (pH 7.1)/50 mM $MgCl_2$ at a temperature of 5°C.

negative band at 248 nm and a slight amplitude decrease and red-shift of the positive bands at 259 nm and 284 nm. The uniqueness of the $(dA)_{10}$:$2(dT)_{10}$ solution CD spectrum provides additional evidence supporting the existence of an unusual DNA structure consisting of three interacting strands.

Imino Proton NMR. The molecular model for triple-helical DNA postulates that one of the two Hoogsteen hydrogen bonds in the T·A·T base triplet involves the thymine N3—H imino proton and the adenine N7 atom (Fig. 4). Under suitable cationic conditions, a second $(dT)_{10}$ strand should form these hydrogen bonds with the $(dA)_{10}$·$(dT)_{10}$ duplex. Consequently, formation of these hydrogen bonds would be accompanied by the induction of additional imino proton resonances in the NMR spectrum. Changes in the imino proton spectrum of a solution containing a 1:2 molar ratio of $(dA)_{10}$ to $(dT)_{10}$ upon titration with $MgCl_2$ are shown in Fig. 5. In the absence of $MgCl_2$, the imino proton resonances (ranging from 13.85 to 14.35 ppm) are identical to those of duplex $(dA)_{10}$·$(dT)_{10}$ (data not shown), indicating that the second equivalent of $(dT)_{10}$ exists in single-stranded form under these conditions. These resonances correspond to thymine N3—H imino protons involved in the standard W–C hydrogen bonding of the duplex. Addition of $MgCl_2$ alters the W–C imino proton resonance pattern, broadens the resonance lines, and simultaneously induces the appearance of new imino proton resonances upfield from where the W–C resonances occurred in the absence of $MgCl_2$ (ranging from 12.50 to 13.70 ppm). Although some of these distinctive upfield resonances may represent W–C base-paired imino protons whose chemical shift has changed upon interaction of duplex $(dA)_{10}$·$(dT)_{10}$ with the second $(dT)_{10}$ strand, others are likely associated with the thymine N3—H imino protons involved in Hoogsteen hydrogen bonding between the second $(dT)_{10}$ strand and the duplex, thereby signifying triplex $(dA)_{10}$·$2(dT)_{10}$ formation. A $MgCl_2$ concentration of 10 mM was sufficient to fully propagate the triplex structure at this DNA concentration (12 mM base = 0.4 mM triplex).

The nonexchangeable proton NMR spectra of a $(dA)_{10}$:$2(dT)_{10}$ sample (at 10 mM $MgCl_2$) and duplex $(dA)_{10}$·$(dT)_{10}$ (at 100 mM NaCl) are quite distinct, with peaks present in the latter spectrum that are completely absent in the former (data not shown). This result shows that no detectable duplex $(dA)_{10}$·$(dT)_{10}$ is present in the $(dA)_{10}$:$2(dT)_{10}$ solution at 10 mM $MgCl_2$. Binding of the third strand to the duplex may alter the overall rigidity of the helix and may thus contribute to the observed line broadening of the imino proton resonances upon addition of the $MgCl_2$. Similar line broadening was also observed in the triplexes stabilized at acid pH (12–14).

Duplex $(dA)_{10}$·$(dT)_{10}$ was also titrated with $MgCl_2$ to a final concentration of 20 mM. After complete melting of the strands following each $MgCl_2$ addition, no new imino proton peaks were seen (data not shown). This result indicates that the presence of triplex-stabilizing concentrations of $MgCl_2$ does not induce the disproportionation of duplex $(dA)_{10}$·$(dT)_{10}$ into triplex and single-strand forms.

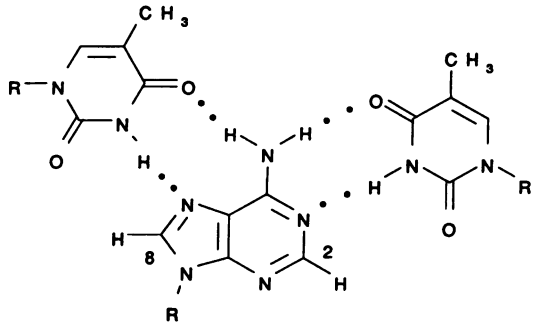

FIG. 4. T·A·T base triplet, indicating both W–C and Hoogsteen hydrogen bonds (· ·).

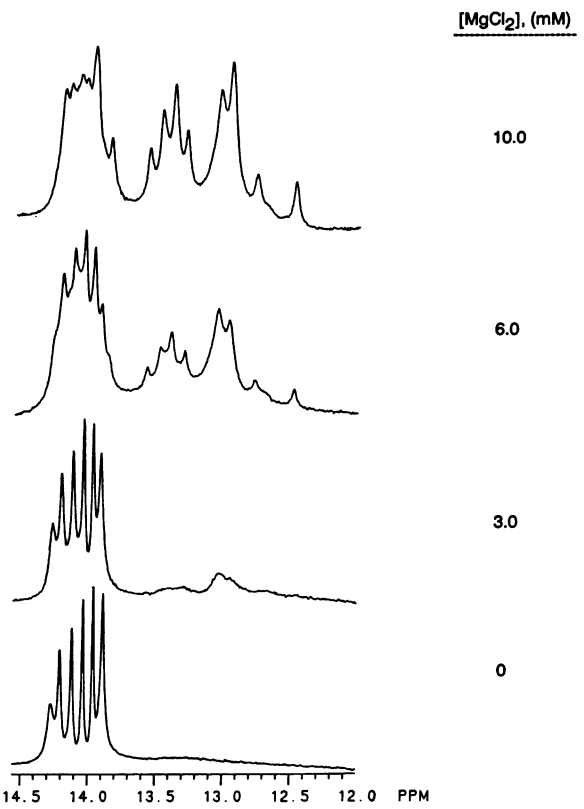

FIG. 5. Imino proton spectra of a $(dA)_{10}$:$2(dT)_{10}$ solution at the indicated concentrations of $MgCl_2$. Experiments were done in 10 mM sodium phosphate (pH 7.1) in 10% D_2O/90% H_2O at 11°C.

Imino Proton–Aromatic Proton NOESY Experiments. Thymine N3—H imino protons involved in standard W–C hydrogen bonding with adenine N1 atoms are known to be dipolar coupled to the nearby adenine C2—H aromatic protons. In the T·A·T base triplet model, the thymine N3—H imino protons involved in Hoogsteen hydrogen bonding with the adenine N7 atoms should be dipolar coupled to the adenine C8—H aromatic protons (see Fig. 4). In an effort to demonstrate this dipolar coupling, two-dimensional NOESY experiments were performed on two distinct Mg^{2+}-stabilized $(dA)_{10}$·$2(dT)_{10}$ triple helices (both at 2 mM triplex concentrations), which only differed with respect to protonation or deuteration at the C8 positions of their $(dA)_{10}$ strands. C8—H deuteration of $(dA)_{10}$ did not alter its ability to form the triplex structure with two equivalents of $(dT)_{10}$, as evidenced by generation of an identical imino proton resonance pattern to that of the undeuterated triplex (data not shown).

Portions of NOESY spectra (250-msec mixing time) of the undeuterated and C8—H-deuterated $(dA)_{10}$·$2(dT)_{10}$ triple helices in 10% D_2O/90% H_2O at 12°C are plotted in Fig. 6. As shown in Fig. 5, triplex stabilization is accompanied by induction of new imino proton resonances upfield (12.50–13.70 ppm) from those of the duplex form (13.85–14.35 ppm). These imino resonances show cross-peaks to adenine aromatic protons, some of which are present in the plots of both the undeuterated (Fig. 6*A*) and C8—H-deuterated (Fig. 6*B*) triplexes and others present in only the undeuterated triplex (denoted by arrows in Fig. 6*A*). Those cross-peaks present in both plots reflect couplings between imino ThyNH3 and aromatic AdeH2 protons, whereas those present in only the undeuterated triplex plot reflect couplings between imino ThyNH3 and aromatic AdeH8 protons. The thymine imino protons showing NOE contacts to AdeH2 protons are thus

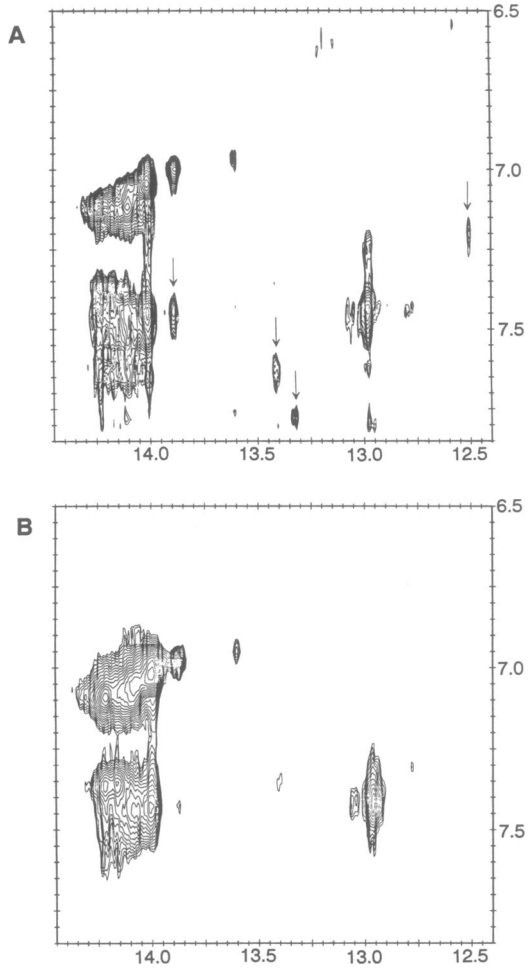

FIG. 6. Portions of the NOESY spectra (250-msec mixing time) of the undeuterated (*A*) and C8—H-deuterated (*B*) $(dA)_{10}\cdot 2(dT)_{10}$ triple helices showing cross-peaks between the ThyNH3 imino and aromatic proton resonances. Arrows in *A* (undeuterated) point out cross-peaks absent in *B* (C8—H-deuterated). Experiments were done in 12 mM sodium phosphate (pH 7.1)/15 mM $MgCl_2$ in 10% D_2O/90% H_2O at 12°C.

engaged in W–C base pairing, whereas those NOE-coupled to the AdeH8 protons are involved in Hoogsteen base pairing. Three resonances corresponding to ThyNH3 imino protons involved in W–C base pairing have shifted upfield as a result of triplex formation, resonating at 12.98, 13.06, and 13.61 ppm in the triplex form. In addition, at least one resonance (13.89 ppm) corresponding to a ThyNH3 Hoogsteen base-paired imino proton emerged within the duplex imino proton region and overlaps a W–C base-paired imino proton.

Strong cross-peaks are also present between adenine aromatic protons in the 6.90- to 7.25- and 7.35- to 7.65-ppm regions and ThyNH3 imino protons in the 13.95- to 14.35-ppm regions of the plots of both the undeuterated (Fig. 6*A*) and the C8—H-deuterated (Fig. 6*B*) triplexes. Although spectral overlap in these regions makes it impossible to resolve individual resonances clearly, the overall peak intensity in these regions is smaller for the deuterated sample. This result suggests that both W–C and Hoogsteen base-paired imino protons resonate in the 13.95- to 14.35-ppm region. The chemical shifts of the resolvable imino ThyNH3 protons engaged in either type of base pairing and the adenine aromatic protons to which they are coupled are summarized in Table 1.

Renewed interest in DNA triple helices has been recently kindled due to suggestions that these structures exist *in vivo*

Table 1. Resolvable proton chemical shifts in the $(dA)_{10}\cdot 2(dT)_{10}$ triplex in H_2O

W–C base pairing		Hoogsteen base pairing	
ThyNH3	AdeH2	ThyNH3	AdeH8
12.98	7.46	12.51	7.22
13.06	7.47	13.33	7.79
13.61	6.99	13.42	7.62
13.89	7.01	13.89	7.46

(22, 23) and the potential for therapeutic applications in which gene expression is repressed by triplex formation (7). Thus, it is important to further our understanding of the physicochemical and structural properties of these nucleic acid forms. We have presented UV, CD, and NMR evidence showing that $MgCl_2$ (at neutral pH) will induce and stabilize a $(dA)_{10}\cdot 2(dT)_{10}$ triple helix, in which the second $(dT)_{10}$ strand interacts with the underlying W–C base-paired $(dA)_{10}\cdot(dT)_{10}$ duplex via Hoogsteen base pairing. Chemical and environmental factors, such as pH, temperature, supercoiling, physiologically relevant cations, mutagens, and other ligands may have different effects on the induction and stability of triple helices. Additional studies on both synthetic and naturally occurring homopurine–homopyrimidine sequences will be necessary to address these issues.

We thank Dr. Roland Brousseau of the Biotechnology Research Institute, Montreal, for help with the synthesis and purification of the oligonucleotides. We also thank Drs. Debra Banville and Burt Feuerstein for helpful discussions. This work was supported by U.S. Public Health Service Grant CA27343, awarded by the National Cancer Institute, and Training Grant GM08284-01, awarded by the National Institute for General Medical Sciences, Department of Health and Human Services.

1. Felsenfeld, G., Davies, D. R. & Rich, A. (1957) *J. Am. Chem. Soc.* **79,** 2023–2024.
2. Riley, M., Maling, B. & Chamberlin, M. J. (1966) *J. Mol. Biol.* **20,** 359–389.
3. Morgan, A. R. & Wells, R. D. (1968) *J. Mol. Biol.* **37,** 63–80.
4. Mirkin, S. M., Lyamichev, V. I., Drushlyak, K. N., Dobrynin, V. N., Filippov, S. A. & Frank-Kamenetskii, M. D. (1987) *Nature (London)* **330,** 495–497.
5. Moser, H. E. & Dervan, P. B. (1987) *Science* **238,** 645–650.
6. Praseuth, D., Perrouault, L., Le Doan, T., Chassignol, M., Thuong, N. & Hélène, C. (1988) *Proc. Natl. Acad. Sci. USA* **85,** 1349–1353.
7. Cooney, M., Czernuszewicz, G., Postel, E. H., Flint, S. J. & Hogan, M. E. (1988) *Science* **241,** 456–459.
8. Arnott, S. & Selsing, E. (1974) *J. Mol. Biol.* **88,** 509–521.
9. Arnott, S., Chandrasekaran, R., Hukins, D. W. L., Smith, P. J. C. & Watts, L. (1974) *J. Mol. Biol.* **88,** 523–533.
10. Arnott, S., Bond, P. J., Selsing, E. & Smith, P. J. C. (1976) *Nucleic Acids Res.* **3,** 2459–2470.
11. Letai, A. G., Palladino, M. A., Fromm, E., Rizzo, V. & Fresco, J. R. (1988) *Biochemistry* **27,** 9108–9112.
12. Rajagopal, P. & Feigon, J. (1989) *Nature (London)* **339,** 637–640.
13. Rajagopal, P. & Feigon, J. (1989) *Biochemistry* **28,** 7859–7870.
14. Santos, C. D. L., Rosen, M. & Patel, D. (1989) *Biochemistry* **28,** 7282–7289.
15. Chamberlin, M. J. (1965) *Fed. Proc. Fed. Am. Soc. Exp. Biol.* **24,** 1446–1457.
16. Job, P. (1928) *Anal. Chim. Acta* **9,** 113–134.
17. Hore, P. J. (1983) *J. Magn. Reson.* **54,** 539–542.
18. States, D. J., Harberhorn, R. A. & Ruben, D. J. (1982) *J. Magn. Reson.* **48,** 286–292.
19. Boelens, R., Scheek, R. M., Dijkstra, K. & Kaptein, R. (1985) *J. Magn. Reson.* **62,** 378–386.
20. Pearson, G. A. (1977) *J. Magn. Reson.* **27,** 265–272.
21. Basus, V. J. (1984) *J. Magn. Reson.* **60,** 138–142.
22. Lee, J. S., Burkholder, G. D., Latimer, L. J. P., Haug, B. L. & Braun, R. P. (1987) *Nucleic Acids Res.* **15,** 1047–1061.
23. Wells, R. D., Collier, D. A., Hanvey, J. C., Shimizu, M. & Wohlrab, F. (1988) *FASEB J.* **2,** 2939–2949.